Carbohydrate Polymers 105 (2014) 169–176

Contents lists available at ScienceDirect

Carbohydrate Polymers

journal homepage: www.elsevier.com/locate/carbpol

Purification, characterization and promoting effect on wound healing of an exopolysaccharide from *Lachnum* YM405

Yunlong He, Ming Ye*, Zhanzhan Du, Huiyan Wang, Yanna Wu, Liu Yang

School of Biotechnology and Food Engineering, Hefei University of Technology, Hefei 230009, China

ARTICLE INFO

Article history:
Received 9 November 2013
Received in revised form 22 January 2014
Accepted 23 January 2014
Available online 3 February 2014

Keywords:
Lachnum
Heteropolysaccharide
Purification
Structural characterization
Scald
Wound healing

ABSTRACT

An exopolysaccharide (LEP-2b) with molecular weight of 2.8×10^4 Da was isolated from *Lachnum* YM405 and purified by DEAE-cellulose 52, Sepharose CL-6B chromatographic column. It consisted of rhamnose (Rha), mannose (Man), glucose (Glc) and galactose (Gal) in a molar ratio of 1.0:5.0:11.5:12.5. Its backbone consisted of →4)-β-D-Man*p*-(1→, →2)-α-D-Rha*p*-(1→, →6)-β-D-Glc*p*-(1→, and →6)-α-D-Gal*p*-(1→, and three types of branches were composed of →6)-α-D-1-OMe-Man*f*-(2→, →6)-β-D-1-OMe-Man*f*-(2→, →1)-α-D-Gal*p*-(6→, →1)-β-D-Gal*p*-(6→, and →1)-β-D-Glc*p*, which were at O-3 of 1,3,6-linked α-D-Man*p* and O-2, O-3 of the same 1,2,3,6-linked β-D-Glc*p* in the backbone respectively. LEP-2b ointment significantly accelerated the decrustation of the wounded skin, shortened the healing time and increased the water and hydroxyproline contents of the healed skin. Combined with the results of macroscopic and histological observations, we deemed that LEP-2b could inhibit inflammatory reaction of scalded skin, accelerate tissue repair and re-epithelialization, thereby playing a positive role in promoting wound healing.

1. Introduction

Fungal polysaccharides are divided into homopolysaccharides and heteropolysaccharides. Homopolysaccharides contain glucans with β-1,3 glycosidic bonds (Rout, Mondal, Chakraborty, & Islam, 2008) as well as manans with α-1,3 or α-1,2 bonds in their backbones (Zeng, Ming, & Zeng, 2001). Heteropolysaccharides include not only an α-1,6-galactan with mannosyl branches (Sun, Liu, Yang, & Kennedy, 2010) but also intricated heteropolysaccharides like a β-1,3-glucan with mannose, galactose and other residues in its side chains (Tong et al., 2009).

Scalds are a type of very common organism burn injuries caused by hot liquids or gases, which are divided into several types in medical science, such as superficial, superficial partial thickness, deep partial thickness and full thickness scalds. Generally, scalds are superficial or superficial partial thickness burns, but deep partial thickness burns may also result, especially with prolonged contact (Maguire, Moynihan, Mann, Potokar, & Kemp, 2008). Among them, superficial partial thickness scalds usually extend into superficial (papillary) dermis, and the main symptoms are redness with clear blister, intense pain, blanches with pressure (Tintinalli, 2010). It was reported that the viability and proliferation of dermal fibroblast were strongly improved in the presence of *Mimosa tenuiflora* arabinogalactan (Zippel, Deters, & Hensel, 2009), and re-epithelization and wound closure were accelerated respectively by three polysaccharides from *Barbados aloe*, *Opuntia ficus-indica* and *Bletilla striata* (Deng et al., 2010; Luo et al., 2010; Trombetta et al., 2006). Likewise, wound repair could also be improved by fungal polysaccharides via stimulating fibroblast expression of wound growth factor, protecting against burn-induced oxidative damage or preventing progressive burn ischemia in the zone of stasis (Firat et al., 2013; Toklu et al., 2006; Wei, Williams, & Browder, 2002).

Lachnum is a genus of saprophytic fungi in the family *Hyaloscyphaceae*, containing about 250 species (Kirk, Cannon, Minter, & Stalpers, 2008). Recently, we have studied the structures and bioactivities of the polysaccharides from several different strains of *Lachnum* and found that they were all glucans linked by β-(1,3)-glycosidic bonds with activities of lowering blood sugar, anti-aging, reducing blood lipids and protecting liver (Qiu, Ma, Ye, Yuan, & Wu, 2013; Ye, Qiu, et al., 2011; Ye, Chen, et al., 2012). Generally speaking, polysaccharides from different species of microorganisms in the same genus are often different in structure. Whether *Lachnum* polysaccharides can promote healing of scalded skin is unclear. Therefore, *Lachnum* YM405 was adopted in this research, and its exopolysaccharide was purified and characterized. Meanwhile, the effect of the polysaccharides on wound healing in scalded mice was evaluated as well.

* Corresponding author. Tel.: +86 55162901505 8614; fax: +86 55162919368.
E-mail addresses: 845212742@qq.com (Y. He), yeming123@sina.com (M. Ye), 173586166@qq.com (Z. Du), whynot-007@163.com (H. Wang), 912446078@qq.com (Y. Wu), yangliu199@163.com (L. Yang).

0144-8617/$ – see front matter © 2014 Elsevier Ltd. All rights reserved.
http://dx.doi.org/10.1016/j.carbpol.2014.01.080

2. Materials and methods

2.1. Materials

The fruiting bodies of *Lachnum* YM405 collected from Yunnan Province (China) were separated and preserved in Microbial Resource and Application Laboratory of the Hefei University of Technology.

2.2. Reagents and instruments

DEAE-cellulose 52 (Whatman Co.); Sepharose CL-6B (Sigma Chemical Co.); Sephadex G-100 (Pharmacia Co.); Qianglie ointment (for scalds and burns, Changchun Overseas Pharmaceutical Group Co., LTD); TFA (trifluoroacetic acid, analytical grade); other reagents were analytical.

Ointment matrix was prepared with vaseline, glycerin, Tween 80 and water in a mass ratio of 30:7:2:1 according to the literature (Chen, 2010).

Waters-1515 HPLC system (Waters-1515 HPLC pump, refractive index detector Waters-2414, Waters Co.), GC–MS analyzer (Japan Shimadzu Co.), Nicolet 67 FT-IR spectrometer (USA Thermo Nicolet Co.), Bruker Avance AV500 nuclear magnetic resonance spectrometer (NMR) spectrometer (Germany Bruker Co.).

2.3. Experimental animals

Eighty four male Kunming mice, weighed 26 ± 2 g, were provided by Experimental Animal Center of Anhui Medical University (Certificate number: No. 1 license of the Medical Laboratory Animal of Anhui). The mice were kept at 23 ± 2 °C with the humidity of 55 ± 5%, and cultured in a 14 h:10 h light–dark cycle.

2.4. Extraction and purification of LEP (*Lachnum* exopolysaccharide)

Fermentation medium was prepared (glucose 20 g L^{-1}, yeast extract 5 g L^{-1}) according to Ye, Qiu, et al. (2011). The *Lachnum* YM405 was incubated in the medium and fermented at 100 r min^{-1}, 30 °C for 6 d. The fermentation broth was precipitated by ethanol and depigmented by 30% H_2O_2 at 50 °C till the solution was colorless. The solution was deproteinized by Sevage method (Ye, Qiu, et al., 2011) and dialyzed in dialysis bag against tap water and distilled water for 48 h successively. Crude polysaccharides were obtained after freeze-drying at −40 °C for 24 h. A 0.1 g mL^{-1} solution of crude polysaccharides was prepared using double distilled water and loaded into DEAE-cellulose 52 chromatographic column (1.6 cm × 50 cm) eluted by 0, 0.3 and 0.5 M NaCl solutions respectively. The main fraction was collected and injected into Sepharose CL-6B column (1.6 cm × 50 cm), which was eluted by 0.9% NaCl solutions. After the fractionization, the main fraction was gathered.

2.5. Purity and molecular weight (M_W) determination of LEP-2b

The purity of LEP-2b was preliminarily tested by gel (Sephadex G-100) permeation chromatography under a normal pressure. UV absorption values of the eluents in each tube were measured at 280 nm. The purity and M_W of LEP-2b was measured by high performance gel permeation chromatography (HPGPC) with the mobile phase of double-distilled water at a flow rate of 0.5 mL min^{-1} and column temperature of 35 °C. The purity of the sample was judged by the shape and distribution of the peak(s), and the M_W was calculated according to the calibration curve established by standard dextrans (M_W: 4,400; 9,900; 21,400; 43,500; 124,000; 196,000; 401,000 Da).

2.6. Monosaccharide composition analysis of LEP-2b

Dry LEP-2b (5 mg) was hydrolyzed in 2 M TFA at 120 °C for 5 h. The subsequent steps were carried out according to the method of Ye, Qiu, et al. (2011). Temperature programming of capillary column in GC–MS: column temperature was increased from an initial temperature of 50 °C to 180 °C at a rate of 10 °C min^{-1}, and then increased to 300 °C at a rate of 3 °C min^{-1}. The other conditions were the same as the method of Ye, Qiu, et al. (2011).

2.7. Structural analysis of LEP-2b

2.7.1. Periodate oxidation-Smith degradation

By referring to the methods of Linker, Evans, and Impallomeni (2001) and Qiu et al. (2013), (12). Three milligrams of LEP-2b was dissolved in 25 mL 15 mM $NaIO_4$. The solution was placed in the dark for reaction, withdrawn 1 mL every 6 h and underwent a 100-fold dilution with distilled water. After the UV spectrophotometer obtained a stable absorbance at 223 nm, 1 mL reaction mixture was titrated with 0.5 mM NaOH to determine the production of formic acid. Finally, ethylene glycol was added to destroy the excessive periodate.

According to Rout et al.'s (2008) method, 2.0 mL methanol was added in the polysaccharide solution after periodate oxidation. The mixture was shaken and left standing for 2 h. The solution was dialyzed against distilled water for 48 h and concentrated under reduced pressure before addition of 80 mg $NaBH_4$. The mixture was oscillated evenly and left standing in a dark place for 24 h. The solution's pH was adjusted to 5.0 by 0.1 M acetic acid and respectively dialyzed against tap water and distilled water for 24 h, and thereafter evaporated to dryness under reduced pressure. TFA (5.0 mL, 2.0 M) was added to the product which was sealed and hydrolyzed at 120 °C for 2 h. The hydrolysate was evaporated under reduced pressure after addition of 3.0 mL methanol. This process was repeated twice to extirpate the TFA left. The product was processed by drying under reduced pressure for 24 h, and then acetylated by the method of Ye, Qiu, et al. (2011) for GC–MS experiment.

2.7.2. Methylation analysis

According to the method of Needs and Swlvendran (1993), 28.0 mg LEP-2b was dissolved in 0.10 mL water. DMSO (5.0 mL) and molecular sieves 3A (5.0 mg) were then added. The solution was filtered with filter paper into the reaction flask, in which 80 mg NaOH and N_2 were poured later. Ultrasonic treatment was performed at room temperature for 30 min. Before the inflation of N_2 (gas) and ultrasound treatment at 20 °C for 1 h, 1.0 mL CH_3I was added into the flask. N_2 was inflated to remove the remaining CH_3I. The methylation was repeated thrice. The reaction was terminated by adding 2 mL water. The product was neutralized with 25% acetic acid and dialyzed against distilled water for 48 h before freeze drying. The methylated products showed no absorption at 3400 cm^{-1} in IR spectroscopy, indicating that LEP-2b was methylated completely. Subsequently, the methylated LEP-2b was hydrolyzed in 2 M TFA at 120 °C for 3 h. The sample was then acetylated in accordance with Ye, Qiu, et al.'s (2011) method for GC–MS analysis.

2.7.3. Partial acid hydrolysis

In the light of the method used by Tong et al. (2009), (80) mg LEP-2b and 8 mL 0.5 M TFA were added to the tube before sealing. The sample was hydrolyzed at 90 °C for 4 h. The acid left was evaporated by co-distillation with carbinol, and the sample was dialyzed against distilled water for 48 h. Ethanol was added after the solutions inside and outside the dialysis bag were respectively concentrated. The precipitate for the inner component and the supernate for the outer were gathered and methylated

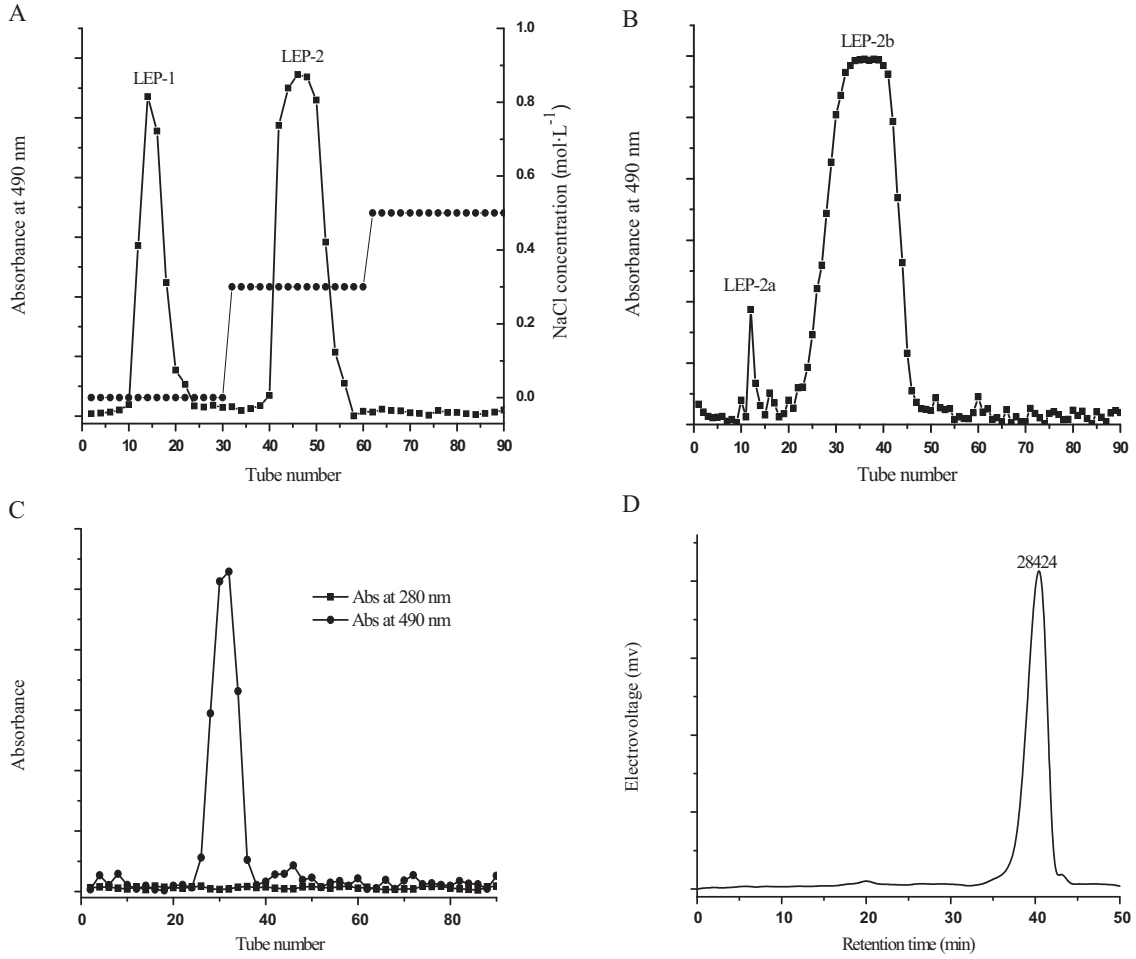

Fig. 1. Chromatograms of LEP on DEAE-cellulose 52 column (A) and Sepharose CL-6B column (B) and chromatograms of LEP-2b on Sephadex G-100 column (C) and HPGPC column (D).

twice separately. The methylated products of them were totally hydrolyzed and acetylized into the corresponding alditol acetates. The product was analyzed by GC–MS according to the method described in Section 2.6.

2.7.4. FT-IR and NMR analysis

According to the literature (Ye, Qiu, et al., 2011), the IR absorption of LEP-2b was measured with KBr pellet (mass ratio 1:100) by FT- IR spectrometer Nicolet 67 within the scanning range of 4000–400 cm^{-1}. NMR spectra were recorded at 500.13 MHz for ^{1}H NMR and 125.76 MHz for ^{13}C NMR on a Bruker AV-500 whose test temperature was set at 27 °C.

2.8. Auxo-action of LEP-2b on wound healing of skins in scalded mice

2.8.1. Establishment, grouping and treatment of scalded mice model

After 1 week of adaptative feeding of the mice, 8% Na_2S alcohol solution was used to depilate the back of the mice to make a glabrous area of 4 cm × 3 cm. The next day, cotton wool dipped in 90 °C hot water was lightly pressed on the back of anesthetized mouse for 5 s to make a burn area of 2 cm^2 (Ren, Guan, Zhao, Ma, & Zhang, 2012). Scalded skin was easily recognized, taking on a whitish and wrinkled appearance, and its subcutaneous tissue showed obvious edema in 3 h, which indicated that the model of superficial partial thickness was successfully established. The mice (84) were randomly and equally divided into six groups including the low-dose group (1% LEP-2b), the high-dose group (3% LEP-2b), negative control group (only applied with ointment matrix), positive control group (treated with Qianglie ointment) and blank control group (scalded mice without any treatment). The skin wounds of the mice in various groups were evenly applied with the same amount (0.2 g) of 1% and 3% LEP-2b ointment twice a day.

2.8.2. Macroscopic assessment and histological observations of the skin wounds

Incrustation and decrustation status of the mice in each group were observed daily and corresponding numbers were recorded to calculate the wound healing time. The wound skins were placed in AAF fixative solution (85 mL 95% ethanol, 10 mL 40% methanal, 5 mL glacial acetic acid) for 1.5 h of fixation and embedded with O.C.T embedding medium (optimum cutting temperature compound); frozen sections (9 μm) of the samples were prepared and stained with Hematoxylin and Eosin (H & E) and observed under optical microscope.

2.8.3. Effect of LEP-2b on water and hydroxyproline (Hyp) contents in scalded skin of the mice

Three mice in each group were sacrificed on days 1, 3, 7 and 18 post-scald. Wounded skin of 1 cm^2 (with thickness of about 1 mm) was taken for each mouse to determine the water (Deng et al., 2010) and Hyp contents (Li & Yao, 2001) in the skins.

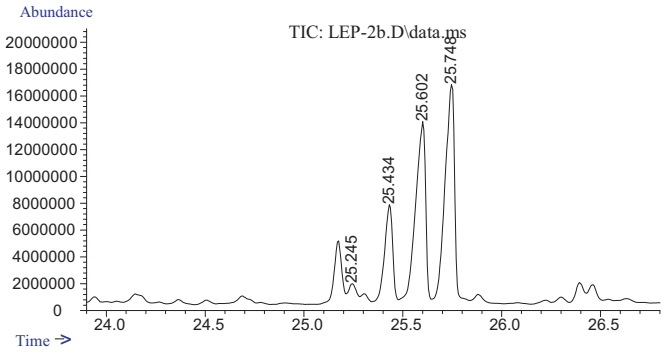

Fig. 2. Total ion chromatogram of acetylated derivatives of total hydrolysate of LEP-2b.

2.8.4. Statistical analysis

All data were processed by DPS v6.55 statistical software and represented as the mean ± standard deviation. The *t*-test analysis was used to analyze the difference between groups. $P < 0.05$ indicated a significant difference, and $P < 0.01$ indicated a very significant difference.

3. Results and discussion

3.1. Purity and molecular weight of LEP-2b

Two fractions designated as LEP-1 and LEP-2 were respectively washed out by double distilled water and 0.3 M NaCl solution from DEAE-Cellulose 52 chromatographic column, without polysaccharide by 0.5 M NaCl aqua (Fig. 1A). LEP-1 from LEP was less than LEP-2, worse still, LEP-1 became much less after the purification by the second column Sepharose CL-6B. Therefore we only studied LEP-2 first. After the purification by Sepharose CL-6B, two fractions were obtained (Fig. 1B), from which the main fraction LEP-2b was chosen. LEP-2b was a water soluble white powder and it contained no proteins or nucleic acid, which was proved by UV spectrum showing no absorption peak at 280 nm and 260 nm.

After LEP-2b was eluted and passed through Sephadex G-100 column, a single elution peak was shown. All absorbance values (A_{280}) of proteins were extremely low and independent of the variation trend of the absorbance (A_{490}) of polysaccharide (Fig. 1C), indicating that LEP-2b was protein-free and was of gel chromatographic grade. HPGPC elution peak in Fig. 1D with narrow distribution was symmetrical, suggesting that the purity of LEP-2b had reached HPLC grade. M_W of LEP-2b was calculated to be 28,424 Da with the equation of the standard curve ($\log M_W = 595 + 93.50T - 11.45T^2 + 0.68T^3$, T represented elution time) and retention time (40.446 min) of the elution peak.

3.2. Structure characterization of LEP-2b

Analysis of acetylated derivative components of the totally hydrolyzed products of LEP-2b by GC–MS software found that four peaks with retention times of 25.245 min, 25.434 min, 25.602 min and 25.748 min on total ion chromatogram (Fig. 2) were obtained. The peaks represented hexaacetates of D-rhamnitol, D-mannitol, D-glucitol and D-galactitol respectively (Chen, Zhang, et al., 2012). Analysis by area normalization method showed that the peak area ratio was about 1.0:5.0:11.5:12.5. In addition, in a failed experiment for monosaccharide analysis performed previously, it was also found by acetylation and GC–MS that the incomplete hydrolysate of LEP-2b contained galactan, β-1,6-glucopyranose, 1-methoxyl-β-D-mannofuranoside and 1-methoxyl-α-D-mannofuranoside. These results showed that LEP-2b was composed of D-rhamnose, β-D-glucopyranose, 1-methoxyl-α-D-mannofuranoside, 1-methoxyl-β-D-mannofuranoside and D-galactose.

Table 1
Data of GC–MS analysis for methylation of LEP-2b, LEP-2bi and LEP-2bo.

Group	Methylated sugar	Linkage	Molar ratio
LEP-2b	2,3,4,6-Me_4-Glc	1-Linked Glc*p*	7.2
	1,3,5-Me_4-Man	2,6-Linked Man*f*	1.9
	2,3,4-Me_3-Glc	1,6-Linked Glc*p*	3.0
	2,3,4-Me_3-Gal	1,6-Linked Gal*p*	15.1
	2,3,6-Me_3-Man	1,4-Linked Man*p*	2.1
	3,4,6-Me_3-Rha	1,2-Linked Rha*p*	1.0
	2,4-Me_2-Man	1,3,6-Linked Man*p*	1.0
	4-Me-Glc	1,2,3,6-Linked Glc*p*	3.0
LEP-2bi	3,4,6-Me_3-Rha	1,2-Linked Rha*p*	1.0
	2,3,6-Me_3-Man	1,4-Linked Man*p*	1.9
	2,3,4-Me_3-Glc	1,6-Linked Glc*p*	3.1
	2,3,4-Me_3-Gal	1,6-Linked Gal*p*	6.2
	4-Me-Glc	1,2,3,6-Linked Glc*p*	2.9
	2,4-Me_2-Man	1,3,6-Linked Man*p*	1.0
LEP-2bo	2,3,4,6-Me_4-Glc	1-Linked Glc*p*	7.0
	2,3,4-Me_3-Gal	1,6-Linked Gal*p*	9.0
	1,3,5-Me_3-Man	2,6-Linked Man*f*	2.0

Results of periodate oxidation showed that 1.00 mol of monosaccharide residue consumed 1.22 mol of periodate and produced 0.533 mol of formic acid. The ratio of IO_4^- consumption to formic acid production was about 2.3:1, indicating that not only a large number of 1 → 6 or 1 → glycosidic bonds, but also 1 → 2, 1 → 4, 1 → 2,6 or 1 → 4,6 glycosidic bonds were present. GC–MS analysis for Smith degradation products showed the presence of a certain amount of mannose, glucose, and a lot of glycerin, indicating that LEP-2b contained a certain amount of glycosidic bonds like 1 → 3, 1 → 3,6, 1 → 2,4 or 1 → 3,4 as well as a large number of 1 → , 1 → 6, 1 → 2 or 1 → 2,6 bonds. The existence of a small amount of erythritol indicated that LEP-2b contained a small amount of 1 → 4 glycosidic bond (Tong et al., 2009). In summary, LEP-2b probably linked by 1 → , 1 → 2, 1 → 3, 1 → 4, 1 → 6,1 → 2,3, 1 → 2,4, 1 → 2,6, 1 → 3,4, 1 → 3,6, 1 → 4,6, etc.

Methylated products of LEP-2b (Table 1) included 2,3,4,6-Me_4-Glc, 1,3,5-Me_3-Man, 2,3,4-Me_3-Glc, 2,3,4-Me_3-Gal, 2,3,6-Me_3-Man, 3,4,6-Me_3-Rha, 2,4-Me_2-Man and 4-Me-Glc with the molar ratio of 7.2:1.9:3.0:15.1:2.1:1.0:1.0:3.0, and the result was consistent with that of the monosaccharide composition analysis. Among which, the presence of 1,3,5-Me_3-Man indicated that LEP-2b contained 2,6-linked Man*f* (mannofuranose). The presence of 2,4-Me_2-Man and 4-Me-Glc indicated that LEP-2b's molecular chains had two branch points at 1,3,6-linked Man*p* (mannopyranose) and 1,2,3,6-linked Glc*p* (glucopyranose). The detection of 2,3,4,6-Me_4-Glc with a large proportion indicated that LEP-2b branch chains commonly terminated with 1-linked Glc*p*.

Methylation analysis of the two components (named as LEP-2bi and LEP-2bo respectively) within and without the bag showed that LEP-2bi, namely the main chain, was formed by 1,2-linked Rha*p*, 1,4-linked Man*p*, 1,6-linked Glc*p*, 1,6-linked Gal*p*, 1,2,3,6-linked Glc*p* and 1,3,6-linked Man*p* with the molar ratio of 1.0:1.9:3.1:6.2:2.9:1.0 (Table 1). Methylates of LEP-2bo contained 1,3,5-Me_3-Man, suggesting that there were furanoid mannosyl residues in the branches. In combination with the monosaccharide composition analysis, C-1 of the Man*f* was connected with —OCH_3. Therefore, the branch chains consisted of 2,6-linked 1-methoxy-Man*f*, 1,6-linked Gal*p* and 1-linked Glc*p* in a molar ratio of 2.0:9.0:7.0 (Table 1).

In the FT-IR spectrum (Fig. 3), a broad peak at 3390 cm^{-1} was caused by the stretching vibration of O—H, and absorption peaks at 2940 cm^{-1} and 1410 cm^{-1} were respectively caused by stretching and bending vibrations of C—H (Chen, Zhang, et al., 2012; Chen, Mao, et al., 2013). The two strong absorptions at

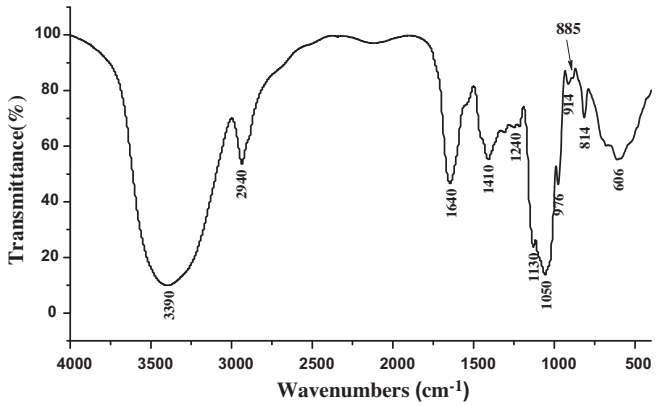

Fig. 3. FT-IR spectrum of LEP-2b.

1130 cm^{-1} and 1050 cm^{-1} indicated that LEP-2b contained pyranose sugar residues, which was verified by the peaks at 914 cm^{-1} and 606 cm^{-1} (respectively caused by asymmetric and symmetric stretching vibrations of pyranoid ring), while the peak at 976 cm^{-1} was caused by the symmetric stretching vibration of furanoid sugar ring (Barker, Bourne, Stacey, & Whiffen, 1954; Wang, Sun, Zhang, Chen, & Liu, 2012). The two peaks at 814 cm^{-1} and 885 cm^{-1} suggested that α- and β-configuration coexisted in LEP-2b (Barker et al., 1954; Wang et al., 2012). The peak at 1640 cm^{-1} was resulted from the bending mode of associated water (Kim, Park, Nam, Lee, & Lee, 2003; Sun & Liu, 2009; Sun et al., 2010).

In the ^{1}H NMR spectrogram (Fig. 4A), the signals within δ 4.50 ~ 4.95 ppm was caused by the anomeric protons of β-configuration sugar residue, and the resonance signals within δ > 4.95 ppm showed that the presence of sugar residues of α-anomeric configuration in LEP-2b. Signals between 3.50 ~ 4.50 ppm were assigned to other protons on the sugar ring. The double peaks (δ 1.23 and 1.22 ppm) near 1.20 ppm and the single peak at 3.13 ppm were signals of protons of methyl in 6-deoxy sugar, namely rhamnosyl residue (Knirel, Shashkov, Senchenkova, Ajiki, & Fukuoka, 2002), and methoxy group in 1-methoxy-mannofuranosyl residue respectively, which were corresponding to the two peaks at 21.58 ppm and 55.52 ppm in ^{13}C NMR spectrum (Knirel et al., 2002; Vinogradov & Wasser, 2005) (Fig. 4B).

In the anomeric region of ^{13}C NMR spectrum (Fig. 4B), the signals at 109.22 ppm and 108.50 ppm represented the anomeric carbon of β-D-1-OMe-Man*f* and α-D-1-OMe-Man*f* (Chen, Zhang, et al., 2012). The signal peak at 103.70 ppm was assigned to anomeric carbons of β-D-Glc*p* and β-D-Man*p* in common, and the resonance at 102.05 ppm was caused by anomeric carbons of β-D-Gal*p* together with α-D-Man*p* (Nandan, Sarkar, Bhanja, Sikdar, & Islam, 2011; Patra et al., 2013). The weak peak at 100.87 ppm was the anomeric carbon signal of α-D-Rha*p* (Knirel et al., 2002). The peak at 99.73 ppm was caused by α-D-Gal*p* (Vinogradov & Wasser, 2005). The presence of signals between δ 82 and 88 ppm indicated the presence of furanoid residues in LEP-2b (Bushmarinov et al.,

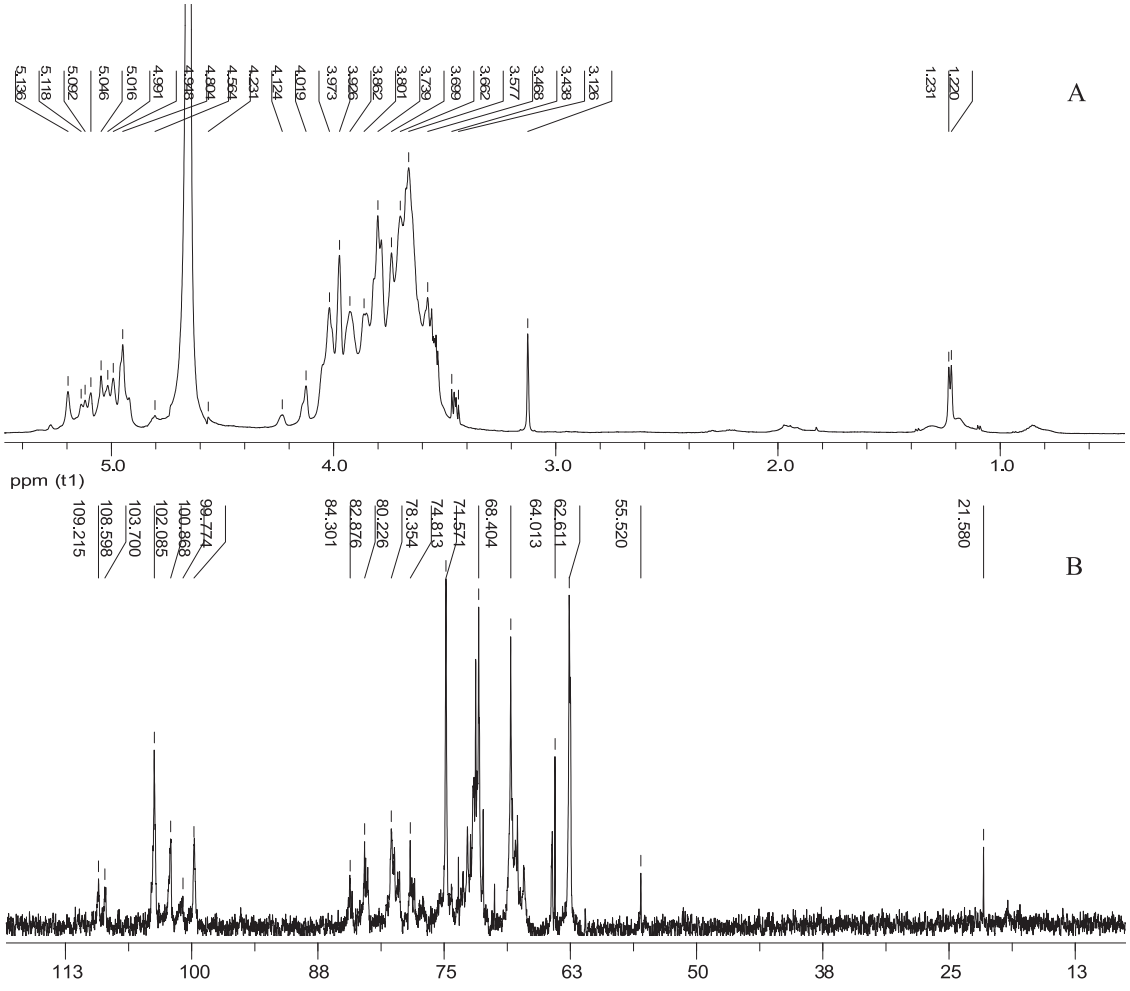

Fig. 4. ^{1}H NMR (A) and ^{13}C NMR (B) spectra of LEP-2b.

Table 2
^{13}C NMR chemical shift (unit: ppm) data of LEP-2b.

Residue	C-1	C-2	C-3	C-4	C-5	C-6
I → 4)-β-Man*p*-(1 →	102.05	80.23	72.68	80.32	71.66	64.01
II → 3,6)-α-Man*p*-(1 →	100.87	68.71	68.71	67.06	71.71	67.45
III → 2)-α-Rha*p*-(1 →	100.99	78.19	71.13	73.66	71.13	21.58
IV → 6)-β-Glc*p*-(1 →	103.83	73.58	84.30	70.00	74.81	68.40
V → 2,3,6)-β-Glc*p*-(1 →	103.59	73.12	84.33	68.56	74.99	67.93
VI → 6)-β-Gal*p*-(1 →	102.08	82.55	78.35	71.57	71.74	68.71
VII → 2)-α-1-OMe-Man*f*-(6 →	108.50	84.12	78.26	82.88	72.38	64.33
VIII → 2)-β-1-OMe-Man*f*-(6 →	109.22	84.30	77.92	82.97	70.06	64.28
IX → 6)-α-Gal*p*-(1 →	99.73	71.50	72.04	71.86	72.14	70.00
X → 1)-β-Glc*p*	103.70	73.58	78.35	71.13	78.02	62.50 and 62.61

2004). Assignments of other carbons (C-2 ~ C-6) were shown in Table 2.

These results showed that LEP-2b possibly had the following repeat unit:

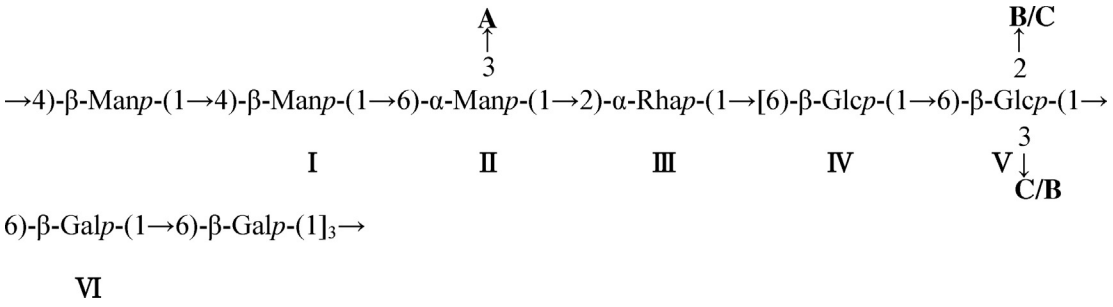

The branches were:

A: 6)-α-1-OMe-Man*f*-(2 → 6)-β-1-OMe-Man*f*-(2 → 1)-β-Glc*p*
B: 1)-β-Gal*p*-(6 → 1)-β-Glc*p* or 1)-α-Gal*p*-(6 → 1)-β-Glc*p* **or** 1)-β-Glc*p*
C: 1)-α-Gal*p*-(6 → 1)-α-Gal*p*-(6 → 1)-β-Glc*p* or
1)-α-Gal*p*-(6 → 1)-β-Gal*p*-(6 → 1)-β-Glc*p* or
1)-α-Gal*p*-(6 → 1)-α-Gal*p*-(6 → 1)-β-Gal*p*-(6 → 1)-β-Glc*p*

3.3. Auxo-action of LEP-2b on skin wound healing in scalded mice

3.3.1. Macroscopic assessment and histopathological observations of the wounds

Redness and swelling with blisters of the scalded skin were observed in depilated Kunming mice treated with 90 °C hot water (Fig. 5(a) A). On day 3 post-scald, scabs were darkened and completely formed in all mice in the high-dose and the low-dose groups. On day 7 post-scald, decrustation had been observed in mice of the low-dose group, and almost complete decrustation was observed in the mice of the high-dose group and positive control group (Fig. 5(a) E and F). On day 18 post-scald, complete decrustation was observed in the injured skin of each mouse, and the skin was covered by new hair. The healing time of the wounded skins of mice in the high-dose group was significantly shortened compared with that in negative control group ($P < 0.05$), and it was not significantly different from that in positive control group.

On day 1 post-scald, inflammatory cell infiltration was relatively mild in the high-dose group (Fig. 5(b) B_1), suggesting that LEP-2b could effectively inhibit inflammation. On day 18, the skin section of the high-dose group (very similar to that of the positive control group) showed well rearranged both epidermis and derma with clear and legible layers, and frequent new capillary vessels (Fig. 5(b) B_{18}, C_{18}, D_{18}, indicated by white arrows). These results were similar with the findings of Trombetta et al. (2006).

Meanwhile, the study found that, on day 18 post-scald, the thickness of the epidermis of mice in the high-dose group was very approximately equal to that of normal mice.

3.3.2. Effect of LEP-2b on water and Hyp contents in scalded skins of the mice

On day 7 post-scald, the water content in wounded skins of mice in the high-dose and low-dose groups was increased compared with that on day 3. Of the two groups, the high-dose group had a significant increase in water content, which was similar to the positive control group. On day 18 post-scald, the water content in wounded skins of the scalded mice was basically the same with that of the non-scalded healthy mice.

As shown in Table 3, the Hyp content in the skins of mice in the low-dose group was significantly increased, and that in the high-dose group was increased very significantly. On day 18 post-scald, the Hyp contents in the skins of mice in the high-dose group and positive control group were both significantly higher than that in negative control group, and the Hyp content in the high-dose group

Table 3
Effect of LEP-2b on healing time, weight gain, water and Hyp contents in scalded skins of the mice.

Group	Healing time (d)	Weight gain (g)	Water content (%)/Hyp content (mg g^{-1})			
			1 d	3 d	7 d	18 d
A	15.14 ± 1.47	9.00 ± 0.49	70.0 ± 1.3/2.17 ± 0.17	65.7 ± 1.7/2.17 ± 0.21	67.0 ± 1.9/2.32 ± 0.19	68.8 ± 1.0/2.32 ± 0.10
B	15.00 ± 1.43	8.27 ± 0.61	67.1 ± 1.6/2.21 ± 0.11	66.3 ± 2.1/2.32 ± 0.10	67.2 ± 1.3/1.99 ± 0.16	68.8 ± 0.7/2.20 ± 0.18
C	13.86 ± 1.35	7.70 ± 0.76	67.1 ± 1.9/2.46 ± 0.17	65.8 ± 2.1/2.40 ± 0.18	67.6 ± 1.0/2.58 ± 0.12[a]	68.9 ± 0.3/2.46 ± 0.12
D	13.00 ± 1.22[a]	11.37 ± 0.91[a]	67.9 ± 1.3/2.69 ± 0.18[a]	63.9 ± 0.7/2.71 ± 0.12[a]	68.9 ± 0.8/2.98 ± 0.10[b]	73.2 ± 1.2[b]/3.03 ± 0.25[b]
E	12.71 ± 1.20[a]	6.01 ± 0.49[b]	69.7 ± 0.6/2.43 ± 0.16	63.6 ± 1.0/2.35 ± 0.09	68.8 ± 0.4/2.54 ± 0.12[a]	73.8 ± 0.6[b]/2.96 ± 0.11[b]

Notes: A. Blank control group; B. Negative control group; C. Low-dose group (1% LEP-2b); D. High-dose group (3% LEP-2b); E. Positive control group.
[a] $P < 0.05$ means a significant difference.
[b] $P < 0.01$ means a very significant difference.

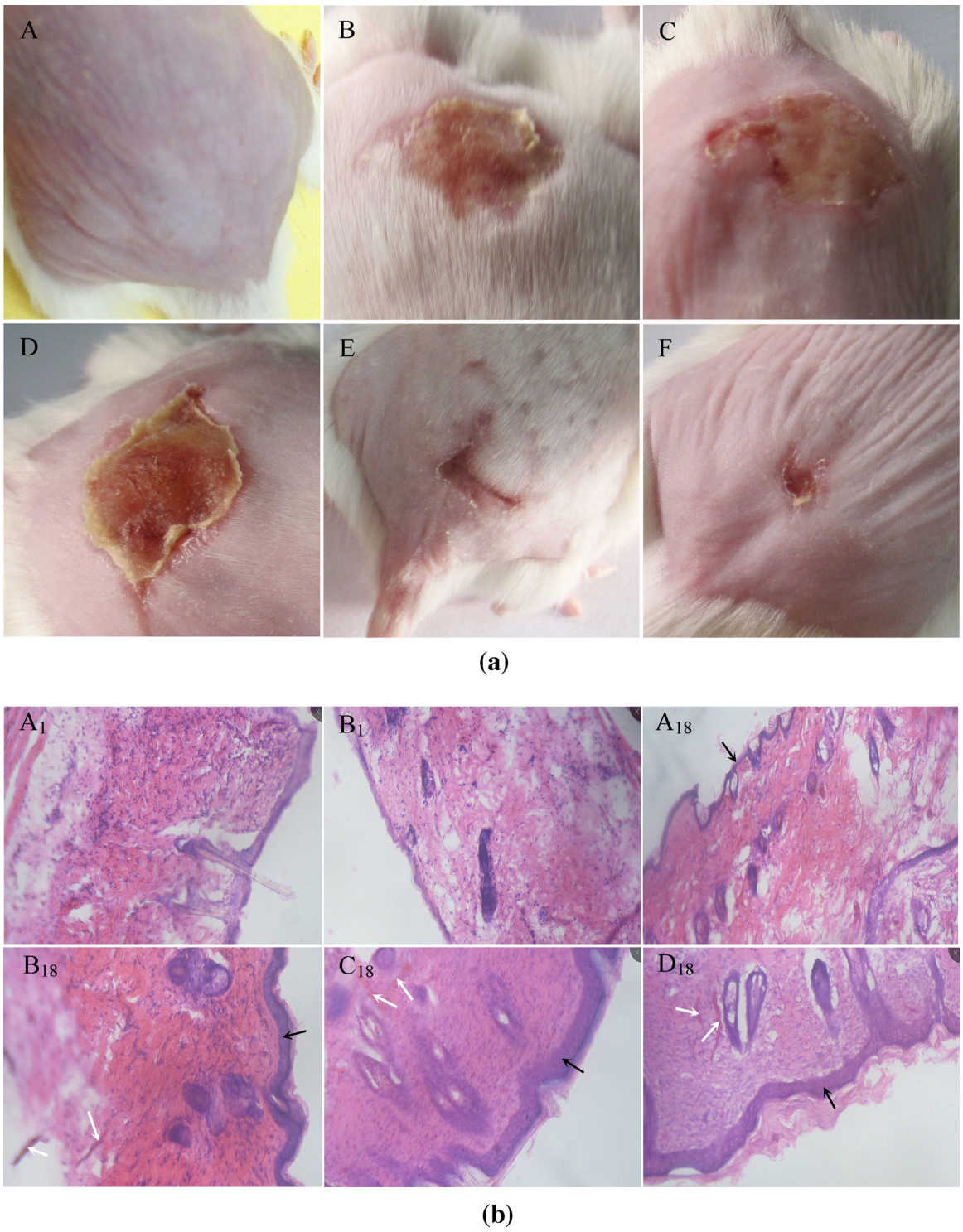

Fig. 5. Appearance and sections of the scalded skin of mice: (a). Appearance of the scalded skin of mice at 1 h post-scald (A) and the skin treated with LEP-2b on day 7 post-scald; B. Blank control group, C. Negative control group, D. Low-dose group (1% LEP-2b), E. High-dose group (3% LEP-2b), F. Positive control group; (b). The skin sections of mice treated with LEP-2b on days 1 and 18 post-scald; A. Blank control group, B. High-dose group (3% LEP-2b), C. Positive control group D. Non-scalded healthy mouse; × 40.

was not significantly different from that in the positive control group.

Compared with the negative control group, during the promotion of the wound healing of scalded mice, LEP-2b simultaneously played a role in increasing the body weight of the mice (Table 3), which was possibly due to glucose uptake and utilization of adipose cells, and expression of determination factor peroxisome proliferator-activated receptor γ in adipose cells that would further improve differentiation of preadipocyte and accumulation of lipid in the cells (Argmann, Cock, & Auwerx, 2005; Liu, Wang, Chen, & Yin, 2007; Wang, Wang, Wang, & Chen, 2004).

Wound healing is an extremely complicated process influenced by a variety of cytokines involved in immune system as well as inflammatory response, vasopermeability. So the immune system plays an important role in it (Feng & Liu, 2012; Park & Barbul, 2004). It is well known that fungal polysaccharides

have immunoregulatory activity (Chen, Zhang, et al., 2012; Sun & Liu, 2009). What's more, *Lachnum* polysaccharides could raise the levels of immunity (Ye, Yuan, He, Du, & Ma, 2013). Therefore, wound healing effect of LEP-2b was strongly connected with its immunoregulatory activity. However, further study is required to clarify the molecular mechanism of LEP-2b's promoting effect on wound healing.

In summary, LEP-2b could inhibit the inflammation in scalded skin, accelerate tissue repair and re-epithelialization and effectively promote the wound healing of scalded skins in mice, which was very likely due to its antioxidative and immunoregulatory activities (Arturson, 1996; Luo et al., 2010; Park & Barbul, 2004; Toklu et al., 2006).

4. Conclusion

The exopolysaccharide LEP-2b ($M_W \approx 2.8 \times 10^4$ Da) from *Lachnum* YM405 consisted of rhamnose, mannose, glucose and galactose, and had three branches respectively substituted at O-3 of Man*p* and O-2, O-3 of the same Glc*p* on the backbone. It was the first heteropolysaccharide isolated from *Lachnum* sp. Composition and configuration of its monosaccharide, types of bonds between the monosaccharides were different from the *Lachnum* polysaccharides (β-glucans) previously studied, suggesting that polysaccharides from different species of *Lachnum* had different structures. LEP-2b was effective in promoting the skin wound healing and it was thus a potential active ingredient of burns drugs.

Acknowledgements

The authors would like to acknowledge the support provided by the project "National Natural Science Foundation of China (31070021)" and the "Fundamental Research Funds for the Central Universities (2012HGZY0020)".

References

Argmann, C. A., Cock, T. A., & Auwerx, J. (2005). Peroxisome proliferator-activated receptor γ: The more the merrier? *European Journal of Clinical Investigation*, *35*(2), 82–92.

Arturson, G. (1996). Pathophysiology of the burn wound and pharmacological treatment. The Rudi Hermans Lecture, 1995. *Burns*, *22*(4), 255–274.

Barker, S. A., Bourne, E. J., Stacey, M., & Whiffen, D. H. (1954). Infra-red spectra of carbohydrates. Part I. Some derivatives of D-glucopyranose. *Journal of the Chemical Society*, 171–176. http://dx.doi.org/10.1039/JR9540000171

Bushmarinov, I. S., Ovchinnikova, O. G., Kocharova, N. A., Blaszczyk, A., Toukach, F. V., Torzewska, A., et al. (2004). Structure of the O-polysaccharide of *Providencia stuartii* O49. *Carbohydrate Research*, *339*(8), 1557–1560.

Chen, G. S. (2010). The preparation of an aloe polysaccharide ointment and the determination of its content. *Clinical Journal of Traditional Chinese Medicine*, *22*(1), 83–84.

Chen, Q., Zhang, S. Z., Ying, H. Z., Dai, X. Y., Li, X. X., Yu, C. H., et al. (2012). Chemical characterization and immunostimulatory effects of a polysaccharide from *Polygoni Multiflori Radix Praeparata* in cyclophosphamide-induced anemic mice. *Carbohydrate Polymers*, *88*(4), 1476–1482.

Chen, Y., Mao, W., Wang, B., Zhou, L., Gu, Q., Chen, Y., et al. (2013). Preparation and characterization of an extracellular polysaccharide produced by the deep-sea fungus *Penicillium griseofulvum*. *Bioresource Technology*, *132*, 178–181.

Deng, S. H., Yang, J. N., Cao, F. J., Cai, X. J., Deng, S. P., & Chen, Y. P. (2010). Accelerating effect for wound healing of *Aloe* polysaccharide on wound tissue of mice with superficial partial-thickness burns. *Lishizhen Medicine and Materia Medica Research*, *21*, 1981–1982.

Feng, Z. K., & Liu, H. (2012). The research progress of wound healing mechanism. *Chinese Journal of Surgery*, *50*(004), 368–372.

Firat, C., Samdancı, E., Erbatur, S., Aytekin, A. H., Ak, M., Turtay, M. G., et al. (2013). β-Glucan treatment prevents progressive burn ischaemia in the zone of stasis and improves burn healing: An experimental study in rats. *Burns*, *39*(1), 105–112.

Kim, G. Y., Park, H. S., Nam, B. H., Lee, S. J., & Lee, J. D. (2003). Purification and characterization of acidic proteo-heteroglycan from the fruiting body of *Phellinus linteus* (Berk. & MA Curtis) Teng. *Bioresource Technology*, *89*(1), 81–87.

Kirk, P. M., Cannon, P. F., Minter, D. W., & Stalpers, J. A. (2008). *Dictionary of the fungi* (10th ed., pp. 358). Wallingford, UK: CAB International.

Knirel, Y. A., Shashkov, A. S., Senchenkova, S. N., Ajiki, Y., & Fukuoka, S. (2002). Structure of the O-polysaccharide of *Pseudomonas putida* FERM P-18867. *Carbohydrate Research*, *337*(17), 1589–1591.

Li, Q. Y., & Yao, R. L. (2001). Determination of hydroxyproline in cells? *Journal of Shanxi Medical University*, *32*(6), 558–559.

Linker, A., Evans, L. R., & Impallomeni, G. (2001). The structure of a polysaccharide from infectious strains of *Burkholderia cepacia*. *Carbohydrate Research*, *335*(1), 45–54.

Liu, Y., Wang, W. J., Chen, W. H., & Yin, J. (2007). Effects of *Astragalus* polysaccharides on proliferation and differentiation of 3T3-L1 preadipocytes. *Journal of Chinese Integrative Medicine*, *5*(4), 421–426.

Luo, Y., Diao, H., Xia, S., Dong, L., Chen, J., & Zhang, J. (2010). A physiologically active polysaccharide hydrogel promotes wound healing. *Journal of Biomedical Materials Research: Part A*, *94*(1), 193–204.

Maguire, S., Moynihan, S., Mann, M., Potokar, T., & Kemp, A. (2008). A systematic review of the features that indicate intentional scalds in children. *Burns*, *34*(8), 1072–1081.

Nandan, C. K., Sarkar, R., Bhanja, S. K., Sikdar, S. R., & Islam, S. S. (2011). Isolation and characterization of polysaccharides of a hybrid mushroom (backcross mating between *PfloVv12* and *Volvariellavolvacea*). *Carbohydrate Research*, *346*(15), 2451–2456.

Needs, P. W., & Swlvendran, R. R. (1993). Avoiding oxidative degradation during sodium hydroxide/methyloidide-mediated carbohydrate methylation in dimethyl suifoxide. *Carbohydrate Research*, *245*, 1–4.

Park, J. E., & Barbul, A. (2004). Understanding the role of immune regulation in wound healing. *American Journal of Surgery*, *187*(5), 11–16.

Patra, S., Patra, P., Maity, K. K., Mandal, S., Bhunia, S. K., Dey, B., et al. (2013). A heteroglycan from the mycelia of *Pleurotus ostreatus*: Structure determination and study of antioxidant properties. *Carbohydrate Research*, *368*, 16–21.

Qiu, T., Ma, X., Ye, M., Yuan, R., & Wu, Y. (2013). Purification, structure, lipid lowering and liver protecting effects of polysaccharide from *Lachnum* YM281. *Carbohydrate Polymers*, *98*, 922–930.

Ren, P., Guan, D. W., Zhao, Y., Ma, W. X., & Zhang, S. T. (2012). Establishment of skin scald model in mice. *Journal of Forensic Medicine*, *28*(2), 92–97.

Rout, D., Mondal, S., Chakraborty, I., & Islam, S. S. (2008). The structure and conformation of a water-insoluble (1 → 3)-, (1 → 6)-β-D-glucan from the fruiting bodies of *Pleurotus florida*. *Carbohydrate Research*, *343*(5), 982–987.

Sun, Y., & Liu, J. (2009). Purification, structure and immunobiological activity of a water-soluble polysaccharide from the fruiting body of *Pleurotus ostreatus*. *Bioresource Technology*, *100*(2), 983–986.

Sun, Y. X., Liu, J. C., Yang, X. D., & Kennedy, J. F. (2010). Purification, structural analysis and hydroxyl radical-scavenging capacity of a polysaccharide from the fruiting bodies of *Russula virescens*. *Process Biochemistry*, *45*(6), 874–879.

Tintinalli, J. E. (2010). *Emergency medicine: A comprehensive study guide*. New York: McGraw-Hill Companies.

Toklu, H. Z., Şener, G., Jahovic, N., Uslu, B., Arbak, S., & Yeğen, B. Ç. (2006). β-Glucan protects against burn-induced oxidative organ damage in rats. *International Immunopharmacology*, *6*(2), 156–169.

Tong, H., Xia, F., Feng, K., Sun, G., Gao, X., Sun, L., et al. (2009). Structural characterization and in vitro antitumor activity of a novel polysaccharide isolated from the fruiting bodies of *Pleurotus ostreatus*. *Bioresource Technology*, *100*(4), 1682–1686.

Trombetta, D., Puglia, C., Perri, D., Licata, A., Pergolizzi, S., Lauriano, E., et al. (2006). Effect of polysaccharides from *Opuntia ficus-indica*(L.) cladodes on the healing of dermal wounds in the rat. *Phytomedicine*, *13*(5), 352–358.

Vinogradov, E., & Wasser, S. P. (2005). The structure of a polysaccharide isolated from *Inonotus levis* P. Karst. mushroom (Heterobasidiomycetes). *Carbohydrate Research*, *340*(18), 2821–2825.

Wang, X. M., Sun, R. G., Zhang, J., Chen, Y. Y., & Liu, N. N. (2012). Structure and antioxidant activity of polysaccharide POJ-U1a extracted by ultrasound from *Ophiopogon japonicus*. *Fitoterapia*, *83*, 1576–1584.

Wang, S. H., Wang, W. J., Wang, X. F., & Chen, W. (2004). Effect of *Astragalus* polysaccharides and berberine on carbohydrate metabolism and cell differentiation in 3T3-L1 adipocytes. *Chinese Journal of Integrated Traditional and Western Medicine*, *24*(10), 926–928.

Wei, D., Williams, D., & Browder, W. (2002). Activation of AP-1 and SP1 correlates with wound growth factor gene expression in glucan-treated human fibroblasts. *International Immunopharmacology*, *2*(8), 1163–1172.

Ye, M., Chen, W. X., Qiu, T., Yuan, R. Y., Ye, Y. W., & Cai, J. M. (2012). Structural characterisation and anti-ageing activity of extracellular polysaccharide from a strain of *Lachnum sp*. *Food Chemistry*, *132*(1), 338–343.

Ye, M., Qiu, T., Peng, W., Chen, W. X., Ye, Y. W., & Lin, Y. R. (2011). Purification, characterization and hypoglycemic activity of extracellular polysaccharides from *Lachnum calyculiforme*. *Carbohydrate Polymers*, *86*(1), 285–290.

Ye, M., Yuan, R. Y., He, Y. L., Du, Z. Z., & Ma, X. J. (2013). Phosphorylation and anti-tumor activity of exopolysaccharide from *Lachnum* YM120. *Carbohydrate Polymers*, *97*(2), 690–694.

Zeng, K. H., Ming, J., & Zeng, K. F. (2001). Structure and function of fungal polysaccharides. *Food Science and Technology*, *4*, 65–68.

Zippel, J., Deters, A., & Hensel, A. (2009). Arabinogalactans from *Mimosa tenuiflora* (Willd.) Poiret bark as active principles for wound-healing properties: Specific enhancement of dermal fibroblast activity and minor influence on HaCaT keratinocytes. *Journal of Ethnopharmacology*, *124*(3), 391–396.